Analysis of SARS-CoV-2 interactions with the Vero cell lines by scanning electron microscopy

Zuzana Malá (zuzana.mala@uhk.cz)
University of Hradec Králové
Marek Vojta
University of Hradec Králové
Jan Loskot
University of Hradec Králové
Radek Sleha
University of Defence in Brno
Bruno Ježek
University of Hradec Králové
Mgr. Josef Zelenka
University of Hradec Králové

Article

Keywords:

Posted Date: April 22nd, 2022

DOI: https://doi.org/10.21203/rs.3.rs-1525580/v1

Abstract

In this study, scanning electron microscopy (SEM) was used to study the cell structure of SARS-CoV-2 infected cells. Our measurements revealed infection remodeling caused by infection, including the emergence of new specialized areas where viral morphogenesis occurs at the cell membrane. Intercellular extensions for viral cell surfing have also been observed. Our results expand our knowledge of SARS-CoV-2 interactions with cells, its spread from cell to cell, and their size distribution. Our findings suggest that SEM is a useful microscopic method for intracellular ultrastructure analysis of cells exhibiting specific surface modifications that could also be applied to studying other important biological processes.

Introduction

The SARS-CoV-2 infection, COVID-19, started in December 2019 in China and has since spread throughout the world[1]. In the Czech Republic, the first cases were reported on March 1, 2020, when SARS-CoV-2 was detected in a passenger entering the Czech Republic from Italy. SARS-CoV-2 is a β-coronavirus from *Coronaviridae* family[1,2]. Coronaviruses are viruses with a single-stranded RNA genome[2], leading generally to a high number of mutations[3,4]. Coronaviruses mainly infect mammals and birds, and can also infect humans and cause respiratory and enteric diseases, such as upper and lower respiratory tract infections (bronchitis, pneumonia, severe acute respiratory syndrome - SARS)[5,6]. According to Bakhshandeh et al.[4], SARS-CoV-2 "*has a relatively high dynamic mutation rate with respect to other RNA viruses*".

Understanding virus-cell interactions provides a crucial basis for the development of vaccines, as well as for the treatment and diagnoses of viral diseases. Up to now, most microscopic studies of SARS-CoV-2 have been carried out by using transmission electron microscopy (TEM)[7], including cryogenic transmission electron microscopy. Pramanick, et al. studied SARS-CoV-2 spike glycoprotein conformations by cryogenic TEM[8]. Scanning electron microscopy is a suitable method for studying, among other things, the interaction of viral particles with the cell surface, changes in its morphology, and dynamics of infection, as shown, e.g., in Caldas et al.[9].

Isolation and rapid sharing of the 2019 novel coronavirus (SARS-CoV-2) from the first patient diagnosed with COVID-19 in Australia was described by Caly et al.[7,10,11,12]. In the presented work, scanning electron microscopy (SEM) was used to study cellular structure of infected cells. Our measurements revealed remodelling of cells caused by the infection, including the emergence of new specialized regions where viral morphogenesis on the cell membrane occurs. Intercellular extensions intended for virus cell surfing were seen too. Our results extend the knowledge of the SARS-CoV-2 interactions with cells and its cell-to-cell propagation.

Material And Methods

Cell line and virus

The wild SARS-CoV-2 strain (kindly provided by Assoc. prof. Daniel Růžek, University of South Bohemia, České Budějovice, Czech Republic) was used in the study. The virus was propagated in Vero cell line CCL81 (Monkey African kidney cell line, purchased from Sigma-Aldrich) that was maintained in Dulbecco's Modified and 100 µg/mL Eagle's Medium (DMEM) with high glucose, containing 10% fetal calf serum, 2 mM glutamine, 100 U/mL penicillin streptomycin (all from Lonza, Swiss). The cells were incubated at 37°C under 5% CO_2 and were observed every 24 hours until 80–90% of the cells exhibited a cytopathic effect (5–7 days). Afterwards, the stock SARS-CoV-2 virus was harvested, and supernatants were collected, aliquoted, and stored at -80°C. All infectious work was performed under biosafety level 3 (BSL3) conditions in the Laboratory of the Department of Epidemiology at the University of Defence, Czech Republic. The microscopic work on the fixed infected Vero cells was performed at the Department of Physics, University of Hradec Králové.

Infection cycle

The Vero cells were seeded on sterile glass coverslips coated with poly-D-Lysine (Merck, USA) in a 24-well plate and incubated at 37°C in 5% CO_2 until 70% confluency was reached. Subsequently, the glasses were infected with SARS-CoV-2 strain at an MOI (multiplicity of infection – the rate of virus per cell) of 0.5 in a 200 µL addition with shaking to distribute the virus. Then the complete medium was added after an absorption period of 1 h at 37°C and 5% CO_2. After that, the plate was incubated under the same conditions for the next 2 days.

Determination of SARS-CoV-2 infectivity by TCID50

The viral titer of SARS-CoV-2 supernatant was determined using an end-point dilution assay and expressed as 50% Tissue Culture Infectious Dose (TCID50)/mL[13]. Briefly, the Vero cells were seeded (20,000 cells per well) onto a 96-well plate (TPP, Swiss) and incubated at 37°C under 5% CO_2 until the confluent monolayer was observed. The tenfold serial dilution of the viral stocks was prepared from 10^{-1} up to 10^{-8}. Subsequently, each dilution of the virus was added to the plate in hexa-plicate. Virus-untreated controls were also included. The plate was then incubated for 5 days at 37°C in 5% CO_2 and the presence of the cytopathic effect was detected under a light microscope. The virus titer was calculated using the method of Spearman and Karber[14].

Scanning electron microscopy

After 48 h post-infection, the coverslips were fixed with 2.5% glutaraldehyde (pH 7.2) for 1 h, washed with phosphate-buffers saline (PBS), and post-fixed in 1% osmium tetroxide (OsO_4) for 40 minutes. After further wash cycles, the samples were dehydrated through an ethanol series (30%, 50%, 70%, 80% 90%, 95%, and 100%, 10 minutes each step). Subsequently, the Vero cells were dried in a critical point dryer CPD300 (Leica, Germany) in liquid CO_2. The dry cells were sputter-coated with a 10 nm thick platinum layer using a sputter coater EM ACE200 (Leica, Germany). Imaging of the samples was conducted by a

scanning electron microscope FlexSEM 1000 (Hitachi, Japan) operated in secondary electrons mode at accelerating voltages of 10 kV, 15 kV, and 20 kV.

SARS-CoV-2 virion size analysis

The aim was to determine the size of the virion particles. Based on SEM observations of SARS-CoV-2-infected Vero cells, the sizes of SARS-CoV-2 virions were quantitatively evaluated. For this purpose, three SEM images were used: ImageA.tif (accelerating voltage: 20 kV, magnification: 18,000×, pixel dimensions: 2,560×1,802 px, scale: 2.757 nm/px, 315 virions processed), ImageB.tif (accelerating voltage: 15 kV, magnification: 30,000×, pixel dimensions: 5,120×3,604 px, scale: 0.833 nm/px, 104 virions processed), and ImageC.tif (accelerating voltage: 15 kV, magnification: 15,000×, pixel dimensions: 5,120×3,604 px, scale: 1.665 nm/px, 196 virions processed). Feret's diameters of the virions presented in these images were measured in ImageJ 1.52a software (imagej.nih.gov/ij/). Each image was initially scaled by assigning the corresponding number of pixels to the given length of its scale bar. To suppress the influence of 3D perspective in the images, only virions located on the upper side of the cells, i.e., horizontally oriented parts of the cell surface, were measured. Feret's diameters were manually marked with the distance measuring tool. In this way, the size distribution of 615 virions coated with a 10 nm thick layer of platinum was obtained.

Results

Scanning electron microscopy showed that the uninfected Vero cells were flat and without distinct surface structures (Fig. 1).

SEM observations of the SARS-CoV-2-infected Vero cells revealed significant changes on their surface induced by the virions (Fig. 2). At the time of their fixation, the individual cells were at different stages of lysis of cell phases of the cycle. A large quantity of extracellular virus was present on the surface of some infected cells. On the other hand, only a few virions were found on other cells, showing an asynchronous infection. Therefore, both damaged cells (Fig. 2C), partially damaged cells (Fig. 2B), and undamaged cells were seen. Furthermore, we observed a large number of vacuoles released during the lysis of virus-infected cells (Fig. 2D).

At higher magnifications, we observed a large number of virus particles (Figs. 3 and 4). The presence of filopodia – protrusions on the cell surface – noticeably increased on the surface of infected cells after infection. The filopodial protrusions on infected cells were also substantially longer and more branched than in the case of uninfected cells. The virus was exported prolifically at the pseudopodia and cell surfaces.

The statistical analysis of SARS-CoV-2 virion sizes revealed that the virion diameters follow a normal (Gaussian) distribution, as shown in Fig. 5. Basic statistical characteristics of the results are given in Table 1.

Table 1
Statistical characteristics of SARS-CoV-2 virion sizes for individual image samples.

	SEM magn.	No. of virions	Mean diameter ± SD (nm)	Std. error (nm)	Median (nm)	95% Confidence interval for the mean (nm)	
						Lower bound	Upper bound
ImageA	18,000×	315	80.52 ± 10.62	0.60	80.32	79.34	81.70
ImageB	30,000×	104	86.68 ± 11.19	1.10	86.28	84.50	88.85
ImageC	15,000×	196	84.47 ± 11.25	0.80	83.48	82.89	86.06

Discussion

The results presented in Fig. 5 and Table 1, obtained from the SEM images ImageA, ImageB, and ImageC, are mutually similar, indicating the reproducibility of the virion size measurements. The lowest standard error was obtained in ImageA, which is probably due to the highest number of evaluated virions in this image. Slight differences in the mean virion diameters between the individual images may be caused by small variations in the focus of the images. The fact that the means are almost equal to the medians gives good evidence of a high symmetry of the measured size distributions.

The determined virion size is in good agreement with other studies: Caldas, et al.[9] reported the diameter of SARS-CoV-2 viruses to be around 70–85 nm, in Zhu et al.[12] the diameters varied from about 60 to 140 nm, in Kim et al.[11] they ranged from 70 to 90 nm, and in Prasad et al.[15] the virion size was around 70–80 nm. Bakhshandeh et al.[4] report a wider range of SARS-CoV-2 virion diameters between 60 and 140 nm.

Unlike us, the cited studies provide only approximate ranges of virion sizes without specifying the distributions of these values. Therefore, it is not possible to directly compare the mean values or medians.

Conclusion

Our data obtained by scanning electron microscopy can provide new insights into the basic SARS-CoV-2/Vero cell interactions and facilitate the identification of targets for the development of preventive and therapeutic strategies to combat infection caused by these viruses. The observations presented should be confirmed and extended by other appropriate biological experiments. However, our findings suggest that SEM is a useful microscopic method for intracellular ultrastructure analysis of cells exhibiting specific surface modifications that could also be applied to studying other important biological processes.

Declarations

Acknowledgements

This work was supported by TAČR GAMA II project Software for virus detection from electron microscopy images and related methodological procedures (TP01010032).

Autor Contributions

Zuzana Malá and Marek Vojta performed the experiments. Josef Zelenka was involved in planning and supervised the experiments. Zuzana Malá processed the experimental data, performed the analysis, drafted the manuscript. Radek Sleha prepared and infected Vero cells by SARS_CoV_2. Jan Loskot and Bruno Ježek performed the statistical analysis. Zuzana Malá wrote the manuscript. All authors discussed the results and contributed to the final manuscript.

Additional Information

The authors declare that they have no known competing financial and non-financial interests or personal relationships that could have appeared to influence the work reported in this paper.

Competing Interests

The authors declare no competing interests.

References

1. Zhu, N., Zhang, D., Wang, W., Li, X., Yang, B., Song, J., Zhao X., Huang B., Shi W., Lu R., Niu P., Zhan F., Ma X., Wang D., Xu W., Wu G., Gao G.F., Phil D. & Tan W. (2020). A novel Coronavirus from patients with pneumonia in China, 2019. New Engl. J. Med.382, 727–733. doi: 10.1056/NEJMoa2001017.
2. Schoeman, D. & Fielding, B. C. (2019). Coronavirus envelope protein: current knowledge. Virology Journal. 16(1), 69. doi: 10.1186/s12985-019-1182-0. PMID: 31133031; PMCID: PMC6537279.
3. Alkhansa, A., Lakkis, G. & El Zein, L. (2021). Mutational analysis of SARS-CoV-2 ORF8 during six months of COVID-19 pandemic. Gene Reports, 23, 101024, doi: org/10.1016/j.genrep.2021.101024.
4. Bakhshandeh, B., Jahanafrooz, Z., Abbasi, A., Goli, M. B., Sadeghi, M., Mottaqi, M. S. & Zamani, M. (2021). Mutations in SARS-CoV-2; Consequences in structure, function, and pathogenicity of the virus. Microbial Pathogenesis, 154, 104831, doi: 10.1016/j.micpath.2021.104831.
5. Peiris, J. S., Guan, Y. & Yuen, K. Y. (2004). Severe acute respiratory syndrome. Nat Med. 10(12 Suppl), S88-S97. doi:10.1038/nm1143.
6. Wang, Y., Li, X., Liu, W., Gan, M., Zhang, L., Wang, J., Zhang, Z., Zhu, A., Li, F., Sun, J., Zhang, G., Zhuang, Z., Luo, J., Chen, D., Qiu, S., Zhang, L., Xu, D., Mok, Ch. K. P., Zhang, F., Zhao, J., Zhou, R. &

Zhao, J. (2020). Discovery of a subgenotype of human coronavirus NL63 associated with severe lower respiratory tract infection in China, 2018, Emerging Microbes & Infections, 9(1), 246–255, doi: 10.1080/22221751.2020.1717999.

7. Caly, L., Druce, J., Roberts, J., Bond, K., Tran, T., Kostecki, R., et al. (2020). Isolation and rapid sharing of the 2019 novel coronavirus (SARS-CoV-2) from the first patient diagnosed with COVID-19 in Australia. Med. J. Aust. 212, 459–462. doi: 10.5694/mja2.50569.
8. Pramanick, I., Sengupta, N., Mishra, S., Pandey, S., Girish, N., Das, A. & Dutta, S. (2021). Conformational flexibility and structural variability of SARS-CoV2 S protein. Structure, 29(8), 834–845.e5, doi: 10.1016/j.str.2021.04.006.
9. Caldas, L.A., Carneiro, F.A., Higa, L.M. et al. (2020). Ultrastructural analysis of SARS-CoV-2 interactions with the host cell via high resolution scanning electron microscopy. Sci. Rep. 10, 16099, doi: 10.1038/s41598-020-73162-5.
10. Colson, P., Lagier, J.-C., Baudoin, J.-P., Bou Khalil, J., La Scola, B. & Raoult, D. (2020). Ultrarapid diagnosis, microscope imaging, genome sequencing, and culture isolation of SARS-CoV-2. Eur. J. Clin. Microbiol. Infect. Dis. 39(8): 1601–1603, doi: 10.1007/s10096-020-03869-w.
11. Kim, J.-M., Chung, Y.-S., Jo, H. J., Lee, N.-J., Kim, M. S., Woo, S. H., et al. (2020). Identification of Coronavirus isolated from a patient in Korea with COVID-19. Osong. Public Health Res. Perspect. 11, 3–7. doi: 10.24171/j.phrp.2020.11.1.02.
12. Zhu, X., Ge, Y., Wu, T., Zhao, K., Chen, Y., Wu, B., Zhu, F., Zhu, B. & Cui, L. (2020). Co-infection with respiratory pathogens among COVID-2019 cases. Virus Research, 285, 198005, https://doi.org/10.1016/j.virusres.2020.198005.
13. Widera, M., Westhaus, S., Rabenau, H. F., Hoehl, S., Bojkova, D., Cinatl, J., Jr, & Ciesek, S. (2021). Evaluation of stability and inactivation methods of SARS-CoV-2 in context of laboratory settings. Medical microbiology and immunology, 210(4), 235–244. doi: 10.1007/s00430-021-00716-3.
14. Spearman, C. The Method of 'Right and Wrong Cases' ('Constant Stimuli') Without Gauss's Formulae. Br. J. Psychol. 1908, 2, 227–242.
15. Prasad, S., Potdar, V., Cherian, S., Abraham, P. & Basu, A.; ICMR-NIV NIC Team (2020). Transmission electron microscopy imaging of SARS-CoV-2. Indian J Med Res. 151 (2&3), 241–243. doi: 10.4103/ijmr.IJMR_577_20. PMID: 32362648; PMCID: PMC7224615.

Figures

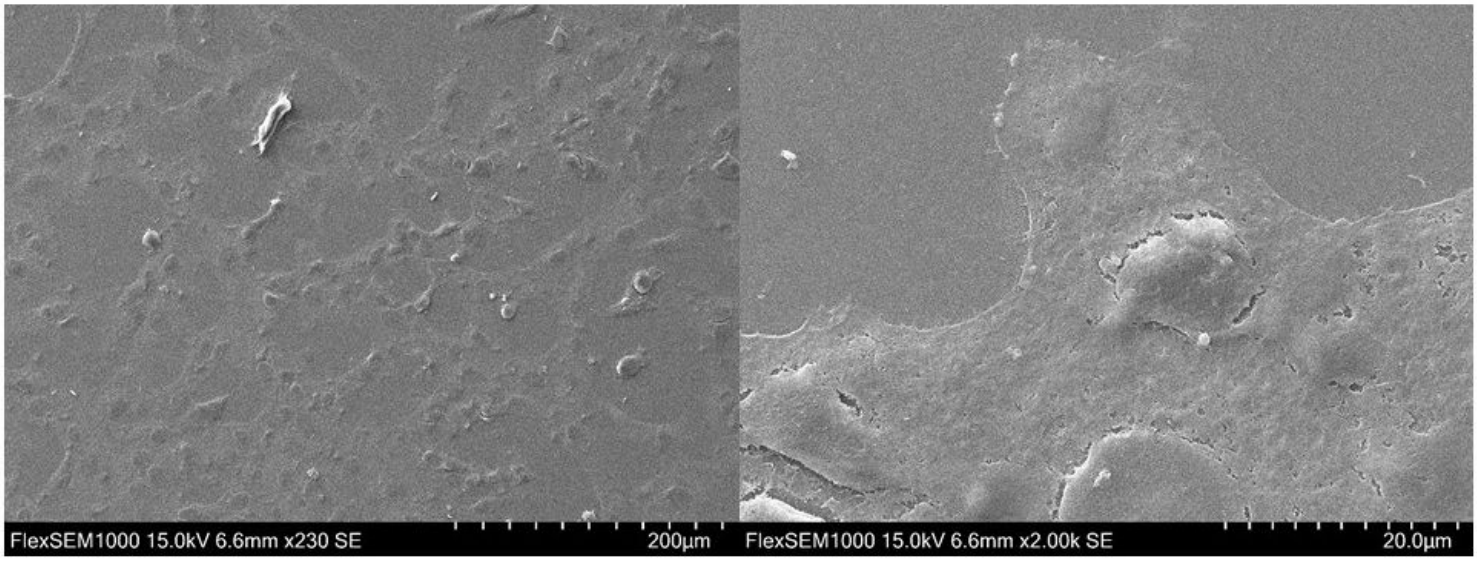

Figure 1

SEM images of uninfected Vero cells. The surface of the cells looks relatively flat with indistinct surface morphology, having no filopodia.

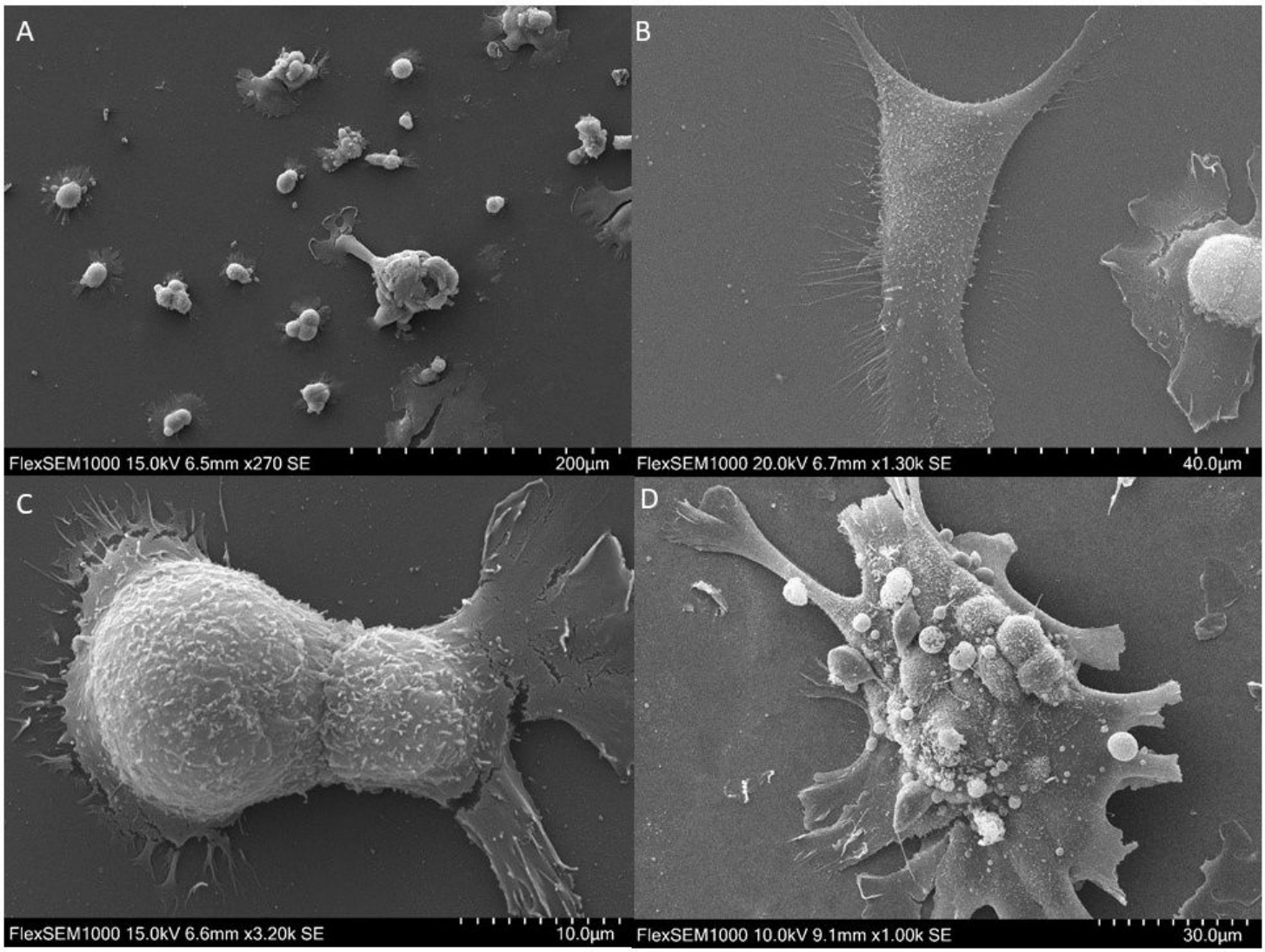

Figure 2

Vero cells infected with SARS-CoV-2 at 24 hours after infection. A: individual Vero cells in different stages of lysis, B and C: partially damaged Vero cell, D: a large number of vacuoles released during the lysis of virus-infected cells

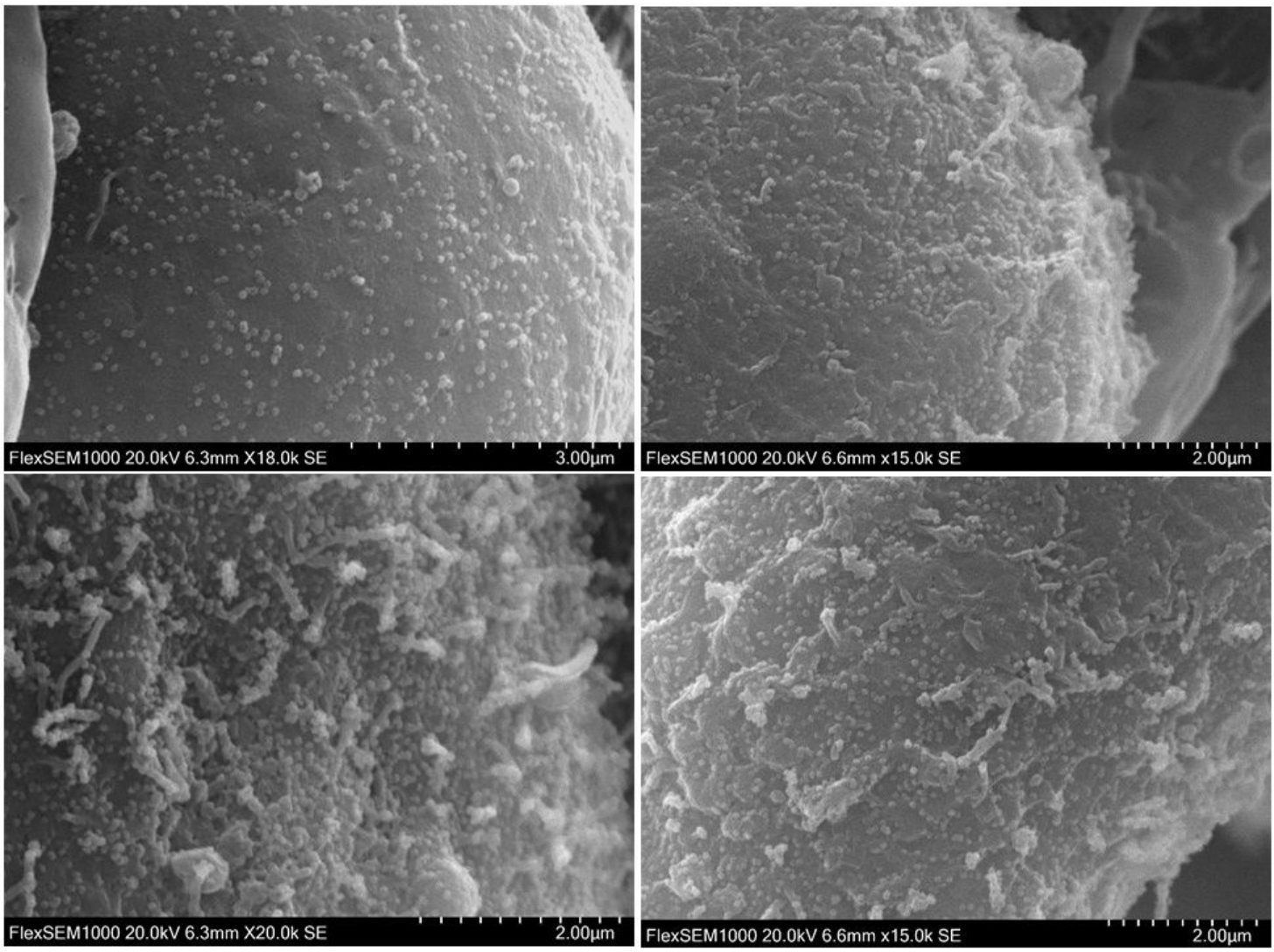

Figure 3

Details of Vero cells infected with SARS-CoV-2. Cell surface is covered with extracellular virus particles.

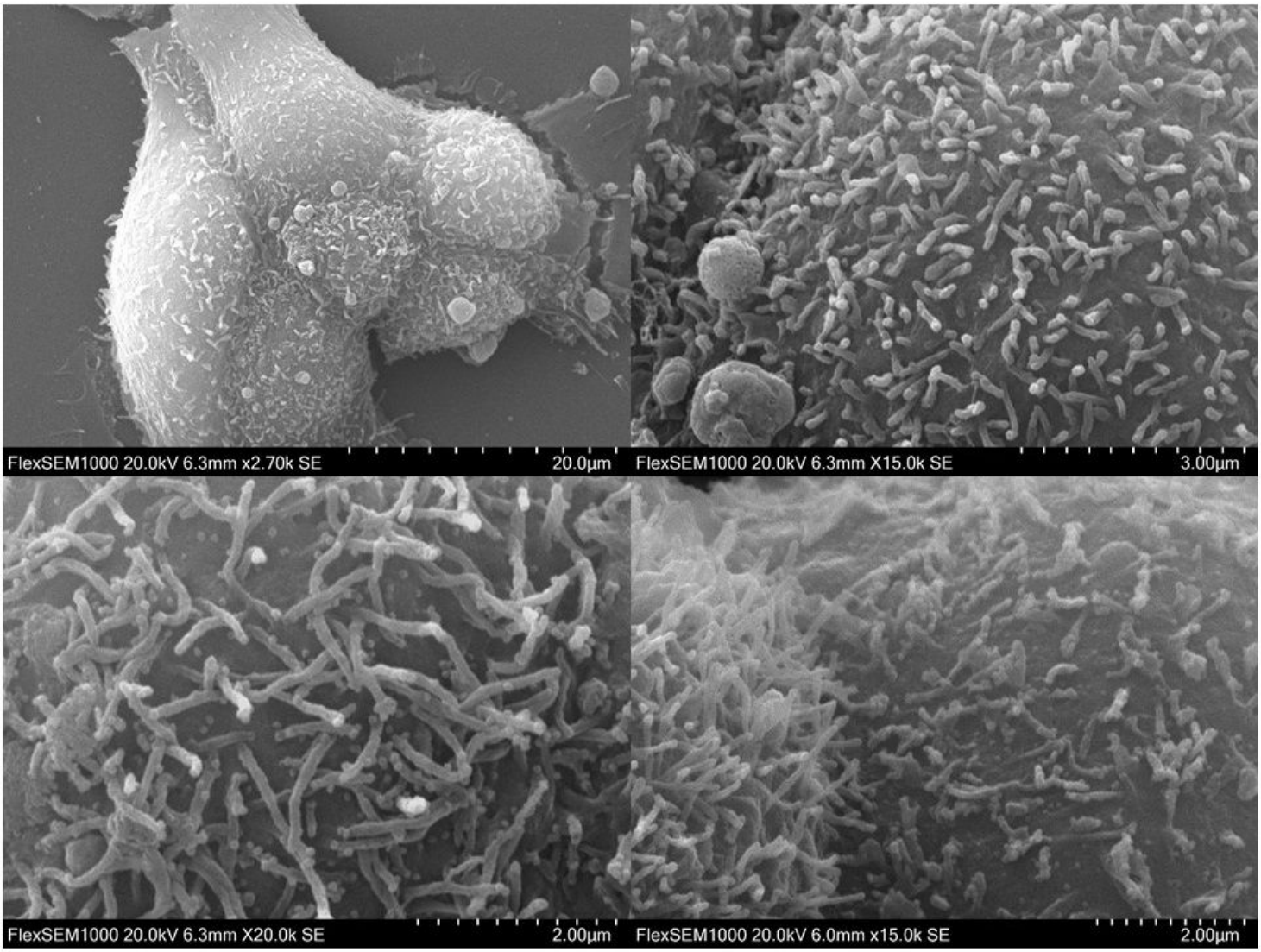

Figure 4

Vero cells infected with SARS-CoV-2. The virions are extruded from or attached to numerous filopodia on the surface of infected cells. A lot of filopodia appear on the surface of infected Vero cells. Some cells appear to have a large amount of extracellular viruses on their surface.

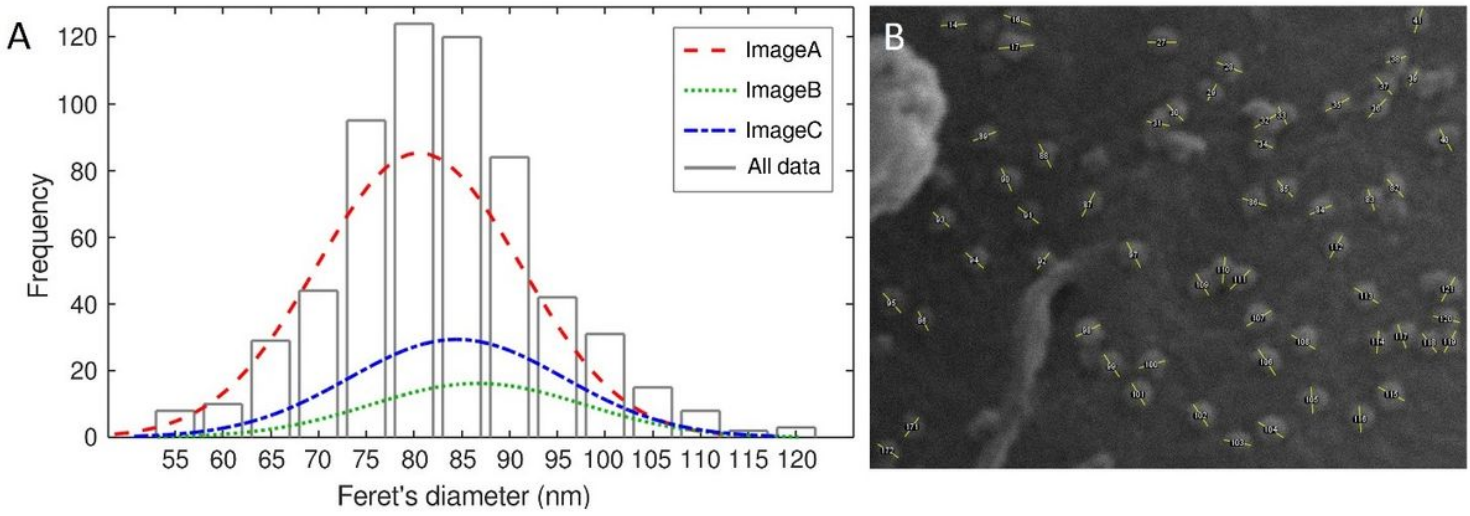

Figure 5

A: A histogram of SARS-CoV-2 virion sizes. The virions were sputter-coated with a 10 nm Pt layer. The vertical bars show the frequencies of values obtained from all 3 images together (ImageA: n=315; ImageB: n=104; ImageC: n=196). The lines show the probability distribution functions for data from the individual images; these functions are scaled by the number of virions measured in the corresponding image. B: A detail of Figure 3A showing the measurement of Feret's diameters of virions in ImageA.

Supplementary Files

This is a list of supplementary files associated with this preprint. Click to download.

- Supplementarydata.docx